

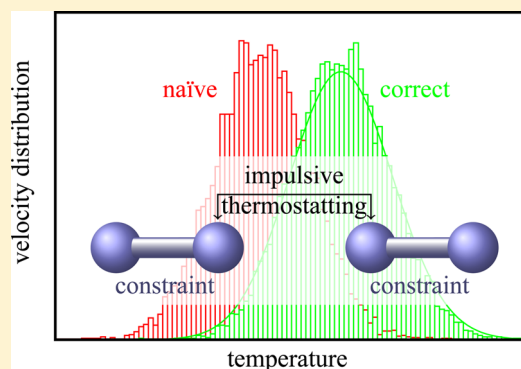
1 Stochastic Dynamics with Correct Sampling for Constrained Systems

2 E. A. J. F. Peters,^{*,†} N. Goga,[‡] and H. J. C. Berendsen[‡]

3 [†]Department of Chemical Engineering and Chemistry, Eindhoven University of Technology, P.O. Box 513, 5600 MB, Eindhoven,
4 The Netherlands

5 [‡]Groningen Biomolecular Sciences and Biotechnology Institute and Zernike Institute for Advanced Materials, University of
6 Groningen, Nijenborgh 7, 9747 AG, Groningen, The Netherlands

7 **ABSTRACT:** In this paper we discuss thermostating using stochastic
8 methods for molecular simulations where constraints are present. For so-called impulsive thermostats, like the Andersen thermostat, the equilibrium
9 temperature will differ significantly from the imposed temperature when a
10 limited number of particles are picked and constraints are applied. We
11 analyze this problem and give two rigorous solutions for it. A correct
12 general treatment of impulsive stochastic thermostating, including
13 pairwise dissipative particle dynamics and stochastic forcing in the
14 presence of constraints, is given and it is shown that the constrained
15 canonical distribution is sampled rigorously. We discuss implementation
16 issues such as second order Trotter expansions. The method is shown to
17 rigorously maintain the correct temperature for the case of SPC/E water
18 simulations.
19



1. INTRODUCTION

20 Stochastic methods have a long history in molecular dynamics
21 simulations.^{1–4} They are used to mimick the nonconservative
22 forces exerted by degrees of freedom that are not explicitly
23 represented in a simplified molecular dynamics (MD) force
24 field. The conservative forces are taken care of by constructing
25 potentials of mean force. The nonconservative forces form a
26 combination of velocity-dependent frictional forces and random
27 components with prescribed correlation in time and space,
28 leading to the *generalized Langevin equation*. The inclusion of
29 correlation in time—while not impossible¹—brings consid-
30 erable additional complications and has not found widespread
31 use. Therefore, we restrict our considerations to random
32 components with white noise character. We allow different
33 friction coefficients for different particles and explicitly allow
34 such combinations of frictions that the resulting dynamics is
35 Galilean-invariant, a requirement for the dynamics to obey the
36 Navier–Stokes relations in the macroscopic limit.

37 While stochastic dynamics was originally designed to
38 faithfully reproduce the dynamics of complex systems with
39 simplified descriptions, its applications have extended to
40 achieve efficient sampling of phase space irrespective of the
41 faithfulness of the generated dynamics. Thus, in *coarse-grained*
42 *dynamics* using superatoms, the phase space sampling will in
43 general be faster without or with reduced stochastic terms. In
44 such systems the inclusion of weak stochastic terms will act as a
45 *thermostat*. It is mandatory that the velocity changes by friction
46 and noise correctly sample a canonical velocity distribution.

47 Many algorithmic implementations of stochastic dynamics
48 involve integration of the stochastic equations of motion over a
49 time step: the influence of friction and noise can be
50 incorporated within the accuracy of the (velocity-)Verlet or

leapfrog algorithms.^{5–7} Such algorithms tend to become rather
51 complex and simplified forms have been devised. 52

53 There is also a second class of stochastic thermostats often
54 used in MD that do not attempt to numerically solve a
55 stochastic differential equation. Examples of such methods are
56 the Andersen⁸ and the Lowe–Andersen⁹ thermostat. In
57 Andersen's method, after performing reversible dynamics
58 driven by the conservative interactions using, for example, a
59 Verlet algorithm, particles are picked and their velocity is reset
60 by drawing a new velocity from the proper Maxwell–
61 Boltzmann distribution. In the Lowe method the same thing
62 is done for the relative velocity of pairs of particles located
63 within a certain cutoff radius from each other. These methods
64 sample the Maxwell–Boltzmann distribution exactly, while
65 having a less well-defined dynamics. 66

67 One can also pick a set of particles or pairs and only partially
68 reset their velocities. In this way an updated velocity is a
69 weighted average of the old value and a random variable. This
70 kind of updating can be performed in such a way that it is a
71 valid discretization of a stochastic differential equation, that is,
72 for $\Delta t \rightarrow 0$ the Langevin equation is recovered. But, in addition,
73 also for finite time steps the Maxwell–Boltzmann distribution is
74 sampled exactly. This approach has been advocated in recent
75 publications.^{10–12} 74

75 We will denote the procedure of picking individual or pairs of
76 particles and (partially) resetting their velocities as *impulsive*
77 application of friction and noise. This kind of thermostating
78 has a large flexibility. One can try to discretize underlying
79 stochastic differential equations faithfully, such as in the case of

Received: May 1, 2014

80 dissipative particle dynamics (DPD).^{10,13} Alternatively, one
81 might be concerned with effective thermalization while not
82 detrimentally influencing the performance of the MD
83 simulation. In this case one can apply, for example, the Lowe
84 thermostat or the impulsive thermostats advocated by Goga et
85 al.¹¹

86 The Andersen thermostat has been widely used and the more
87 novel impulsive thermostats are gaining popularity. In this
88 article we consider the application of these thermostats in the
89 presence of holonomic constraints. It was proven by Ryckaert
90 and Ciccotti¹⁴ that when applying the Andersen thermostat to
91 *all* particles and subsequently applying constraints, the correct
92 velocity distribution is sampled. However, one of the nice
93 features of the nonconstrained Andersen/Lowe thermostat is
94 that one also can pick one particle or a pair or a limited number
95 of particles and rethermalize only these. It turns out that in the
96 presence of constraints, this procedure leads to erroneous
97 results.

98 We find that, when naively applying the impulsive thermo-
99 stats to a subset of all particles, as in a nonconstrained case, and
100 subsequently projecting the velocities according to the imposed
101 constraints, an incorrect velocity distribution is sampled. This
102 can lead to serious deviations of the temperature from the one
103 that one would like to be imposed by the thermostat. This is a
104 not widely acknowledged issue and therefore worthwhile
105 pointing out. We will not only focus attention on this problem
106 but also provide a solution for it.

107 This paper is focused on the handling of constraints for
108 impulsive thermostats. In comparison, for deterministic
109 thermostats (such as Nosé–Hoover) constraints do not impose
110 extra complications, and methods of rigorously handling them
111 are well-known. For constrained Langevin dynamics, however,
112 some proposals in literature have been published.^{15,16} These
113 include second-order schemes, but no schemes that leave the
114 Boltzmann distribution invariant, as an impulsive thermostat
115 does. Most of these papers mainly contain theoretical
116 derivations base on the numerical approximations for stochastic
117 differential equations (SDEs). These papers consider the
118 “simple” Langevin dynamics with a constant friction factor,
119 where the frictional force on a particle is proportional to its
120 velocity. Our method is related, because it can be used for the
121 numerical solution of constrained Langevin equations. How-
122 ever, our method is more general because it also considers a
123 system with dissipative Galilean-invariant pair interactions
124 (DPD) and can be used for impulsive thermostats that are
125 not formulated in terms of an SDE (Andersen and Lowe–
126 Andersen).

127 This article is organized as follows. After recapitulating the
128 theory^{10–12} for impulsive thermostating in unconstrained
129 systems (Section 2), we show two examples where naive
130 application of this theory to constrained systems leads to an
131 equilibrium temperature that deviates from the reference
132 temperature imposed by the thermostat (Section 3). In Section
133 4 we present a formalism for impulsive thermostating, based
134 on a consistent matrix notation. This includes (in Section 4.2)
135 the projection operator that realizes the projection of
136 unconstrained velocities onto the constrained hypersurface.
137 After stating the constrained canonical distribution of Cartesian
138 velocities in Section 4.3, we present the correct handling of
139 impulsive thermostating in the presence of constraints in
140 Section 4.4. This is the main result of this paper.

141 Section 5 discusses the full integration of the equations of
142 motion, including velocity updates by friction and noise and the

possibility of Trotter operator splitting. In Section 6 we show
143 that application of the proper thermostating proposed in
144 Section 4.4 to the examples of Section 2 yields correct results,
145 as does a DPD-type thermostating for rigid SPC/E water using
146 one pair per particle, independent of the strength of the applied
147 friction. Finally, conclusions are discussed in Section 7. 148

2. IMPULSIVE THERMOSTATING FOR UNCONSTRAINED SYSTEMS

149

Impulsive application of friction and noise to a single particle i
150 consists of a velocity reduction (or damping) of the particle,
151 followed by a partial rethermalization to the canonical
152 (Maxwell–Boltzmann) distribution. We assume an isotropic
153 application in three dimensions, although this is not a
154 requirement. 155

Denoting the “old” velocity vector by \mathbf{v}_i and a vector of three
156 independent Gaussian stochastic variables of zero mean and
157 variance 1 by $\boldsymbol{\xi}$, the new velocity \mathbf{v}'_i is given by 158

$$\mathbf{v}'_i = (1 - f)\mathbf{v}_i + g\boldsymbol{\xi} \quad (1) \quad 159$$

$$\langle m_i \mathbf{v}'_i{}^2 \rangle = (1 - f)^2 \langle m_i \mathbf{v}_i{}^2 \rangle + 3m_i g^2 \quad (2) \quad 160$$

Requiring that the kinetic energy obeys the correct
161 equipartition value corresponding to the temperature of the
162 heat bath, $\langle m_i \mathbf{v}'_i{}^2 \rangle = \langle m_i \mathbf{v}_i{}^2 \rangle = 3k_B T$, gives 163

$$g^2 = f(2 - f)k_B T / m_i \quad (3) \quad 164$$

Note that a sum of Gaussian variables gives again a Gaussian
165 variable. Therefore, the stationary distribution is Gaussian with
166 the correct variance, that is, the proper Maxwell–Boltzmann
167 distribution. 168

When explicitly integrating over a finite time-step Δt , the
169 stochastic differential equation corresponding to Langevin
170 dynamics with constant friction: 171

$$m_i d\mathbf{v}_i = -\zeta \mathbf{v}_i dt + \sqrt{2k_B T \zeta} d\mathbf{W}_i \quad (4) \quad 172$$

where \mathbf{W}_i is a three-dimensional Wiener process, one finds that
173 the exact so-called weak solution is given by eq 1 with $f = 1 -$
174 $\exp(-\zeta \Delta t / m_i)$ and $g^2 = (k_B T / m_i)[1 - \exp(-2\zeta \Delta t / m_i)]$. This is
175 an example that obeys relation eq 3. 176

This scheme can straight-forwardly be generalized¹¹ to re-
177 equilibrating relative velocities $\mathbf{v}_{ij} = \mathbf{v}_i - \mathbf{v}_j$ by the substitution \mathbf{v}_i
178 $\rightarrow \mathbf{v}_{ij}$ and $m_i \rightarrow \mu_{ij}$ (reduced mass). In this case the
179 equipartition theorem tells that $\mu_{ij} \mathbf{v}_{ij}{}^2 = 3k_B T$, with $\mu_{ij}^{-1} = 1/$
180 $m_i + 1/m_j$. For pairs of particles the thermostating should leave
181 the center-of-mass velocity (or the total momentum) invariant,
182 such that 183

$$\mathbf{v}'_i = \mathbf{v}_i + (\mu_{ij}/m_i)(\mathbf{v}'_{ij} - \mathbf{v}_{ij}), \quad \mathbf{v}'_j = \mathbf{v}_j - (\mu_{ij}/m_j)(\mathbf{v}'_{ij} - \mathbf{v}_{ij}) \quad (5) \quad 184$$

This implementation is named¹¹ isotropic, since the directions
185 of applied noise are isotropically distributed in three
186 dimensions. 187

One may also apply the friction and fluctuating force only in
188 the direction of the connecting vector (indicated by unit vector
189 $\hat{\mathbf{r}}_{ij}$). In this case we get a one-dimensional *parallel* update of the
190 relative velocity, equivalent to the friction and noise proposed
191 in the original DPD method:¹⁷

$$\mathbf{v}'_{ij} = \mathbf{v}_{ij} - f(\mathbf{v}_{ij} \cdot \hat{\mathbf{r}}_{ij})\hat{\mathbf{r}}_{ij} + g\hat{\mathbf{r}}_{ij}\boldsymbol{\xi} \quad (6) \quad 192$$

193 Also here we find the requirement that $g^2 = f(2-f)k_B T/\mu_{ij}$.
 194 Similarly, a two-dimensional *perpendicular* scheme can be
 195 devised with velocity update in the plane perpendicular to $\hat{\mathbf{r}}_{ij}$.
 196 We refer to Section 4.1 for a more formal description and to ref
 197 11 for explicit algorithms in these cases.

3. TWO EXAMPLES OF NAVE IMPLEMENTATIONS OF CONSTRAINTS

198
 199 In the absence of constraints the equations given above
 200 guarantee that the application of friction and noise to individual
 201 particles or particle pairs drives the actual temperature of the
 202 affected degrees of freedom toward the reference temperature.
 203 Because of kinetic energy transfer resulting from interparticle
 204 forces (thermal conduction) the temperature of the system as a
 205 whole will tend to the reference temperature; hence, such
 206 friction and noise acts as a thermostat.

207 In the presence of constraints this is not the whole story.
 208 After applying friction and noise according to the equations
 209 given above, the velocities will not be constrained and contain
 210 components in directions deviating from the constraint
 211 hypersurface. In practice a *constraint step* is introduced, which
 212 corrects these deviations. While Ryckaert and Ciccotti¹⁴ have
 213 proven that a correct canonical ensemble for the constrained
 214 system is obtained after applying a constraint algorithm to a
 215 system in which *all* degrees of freedom are completely
 216 randomized to a Maxwellian velocity distribution, it is not at
 217 all clear that applying (partial) thermostating constraints to
 218 selected degrees of freedom yields correct temperatures if
 219 constraints are present. In fact, it is clear from studying two
 220 simple examples that this is *not* the case and that noticeable
 221 errors in thermal behavior result.

222 Consider a one-dimensional system of homonuclear diatomic
 223 molecules. Each atom has mass m ; the molecular mass is $2m$.
 224 Consider one particular molecule with atoms 1 and 2 and apply
 225 thermostating to atom 1. This situation is depicted in Figure 1.

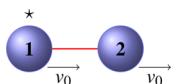


Figure 1. Thermostating a one-dimensional system of homonuclear diatomic molecule. One atom indicated by the star is natively thermostated. After imposing the bond-length constraint the kinetic temperature has a different value from the imposed heat-bath temperature.

226 The molecule (and thus each of the atoms) has an initial
 227 velocity v_0 . Now apply friction and noise to atom 1, yielding
 228 velocities v'_1 and v'_2 :

$$229 \quad v'_1 = (1-f)v_0 + g\xi; \quad v'_2 = v_0 \quad (7)$$

230 where g follows from eq 3. Now apply constraints: in this
 231 simple case the constraints remove the relative velocity, and the
 232 new constrained velocities are equal for both atoms and equal
 233 to the center-of-mass velocity

$$234 \quad v_{\text{cm}} = \frac{1}{2}(v'_1 + v'_2) = v_0 - \frac{1}{2}fv_0 + \frac{1}{2}g\xi \quad (8)$$

235 The new mean-squared velocities are equal to

$$\begin{aligned} \langle v_{\text{cm}}^2 \rangle &= \left(1 - \frac{1}{2}f\right)^2 \langle v_0^2 \rangle + \frac{1}{4}g^2 \\ &= \left(1 - \frac{1}{2}f\right)^2 \langle v_0^2 \rangle + \frac{1}{4}f(2-f)\frac{k_B T}{m} \end{aligned} \quad (9) \quad 236$$

We now look for the equilibrium kinetic temperature T_{kin} that
 the system will attain and for which

$$\langle v_{\text{cm}}^2 \rangle = \langle v_0^2 \rangle = \frac{k_B T_{\text{kin}}}{2m} \quad (10) \quad 239$$

Using eqs 9 and 10 we find

$$T_{\text{kin}} = \frac{1 - \frac{1}{2}f}{1 - \frac{1}{4}f} T \quad (11) \quad 241$$

The equilibrium kinetic temperature is smaller than the
 reference temperature of the heat bath. Thus, the constraint
 algorithm does not properly remove the excess velocity
 generated by friction and noise outside the constraint
 hypersurface. In the case of full randomization of the first
 atom ($f = 1$), the equilibrium temperature is only 2/3 of the
 reference temperature. This is an example of an Andersen
 thermostat applied to a subset of particles in the presence of
 constraints.

As a second example consider a one-dimensional system of
 homonuclear diatomic molecules. Each atom has mass m , so
 the molecular mass is $2m$. Consider two neighboring molecules
 A and B with atoms 1 and 2 and, respectively, 3 and 4. Apply
 DPD friction and noise to particle pair 2–3, see Figure 2.

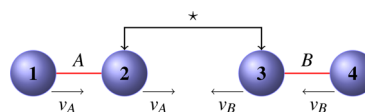


Figure 2. Two one-dimensional homonuclear diatomic molecules with bond-length constraints. A pairwise impulsive thermostating is applied to the particles 2–3.

Molecule A (and thus each of the atoms 1 and 2) has an
 initial velocity v_A . Likewise molecule B with atoms 3 and 4 has
 velocity v_B . Now apply friction and noise to the pair 2–3
 according to the equations given in Section 2. The velocity
 difference $v_{AB} = v_A - v_B$ is modified to

$$v'_{AB} = (1-f)v_{AB} + g\xi \quad (12) \quad 261$$

where the mass that should be used to compute g in eq 3 is the
 reduced mass $\mu_{AB} = m/2$.

The resulting velocity difference is then distributed equally
 between atoms 2 and 3 such that the center-of-mass of 2 + 3 is
 not influenced, yielding

$$\begin{aligned} v'_2 &= \left(1 - \frac{1}{2}f\right)v_A + \frac{1}{2}fv_B + \frac{1}{2}g\xi \\ v'_3 &= \left(1 - \frac{1}{2}f\right)v_B + \frac{1}{2}fv_A - \frac{1}{2}g\xi \end{aligned} \quad (13) \quad 267$$

The next step is application of the constraints, that is,
 constructing the center-of-mass velocity of the molecules:

$$v'_A = \frac{1}{2}(v_A + v'_2) = \left(1 - \frac{1}{4}f\right)v_A + \frac{1}{4}fv_B + \frac{1}{4}g\xi$$

$$v'_B = \frac{1}{2}(v'_3 + v_B) = \left(1 - \frac{1}{4}f\right)v_B + \frac{1}{4}fv_A - \frac{1}{4}g\xi \quad (14)$$

271 If we evaluate the second moments this gives

$$\langle v_A^2 \rangle' = \left(1 - \frac{1}{4}f\right)^2 \langle v_A^2 \rangle + \frac{1}{16}f^2 \langle v_B^2 \rangle + \frac{1}{2}f \left(1 - \frac{1}{4}f\right) \langle v_A v_B \rangle + \frac{1}{16}g^2$$

$$\langle v_A v_B \rangle' = \frac{1}{4}f \left(1 - \frac{1}{4}f\right) (\langle v_A^2 \rangle + \langle v_B^2 \rangle) + \left[\left(1 - \frac{1}{4}f\right)^2 + \frac{1}{16}f^2 \right] \langle v_A v_B \rangle - \frac{1}{16}g^2 \quad (15)$$

272 where the equation for $\langle v_B^2 \rangle'$ is the same of that of $\langle v_A^2 \rangle'$ with
273 indices A and B interchanged. If the thermostat is applied
274 multiple times finally a fixed point is reached for the Gaussian
275 velocity distribution with $\langle v_A^2 \rangle' = \langle v_B^2 \rangle' = \langle v_A^2 \rangle' = \langle v_B^2 \rangle'$ and
276 $\langle v_A v_B \rangle' = \langle v_A v_B \rangle$. This gives,

$$\langle v_A^2 \rangle = \frac{g^2}{8f \left(1 - \frac{1}{4}f\right)} = \frac{1 - \frac{1}{2}f}{1 - \frac{1}{4}f} \frac{k_B T}{2m}; \quad \langle v_A v_B \rangle = 0 \quad (16)$$

279 such that

$$T_{\text{kin}} = \frac{1 - \frac{1}{2}f}{1 - \frac{1}{4}f} T \quad (17)$$

281 As in the Langevin case the equilibrium temperature is lower
282 than the reference temperature, especially if f deviates
283 significantly from 0.

284 The main conclusion is that a naive implementation of
285 impulsive thermostats such as the Andersen, Lowe–Andersen,
286 DPD thermostat of Peters, or the family of thermostats
287 proposed by Goga et al. will, if constraints are present, give rise
288 to a systematic deviation of the computed kinetic temperature
289 from the imposed heat-bath temperature. How serious this
290 deviation is depends on the magnitude of f and on the sequence
291 of thermostating operations followed by the application of
292 constraints.

4. FORMALISM FOR IMPULSIVE THERMOSTATING

293 In this section we will formally describe impulsive thermo-
294 statting using matrix notation. The central point is the velocity
295 correlation matrix that follows from the equipartition theorem
296 of statistical mechanics; the thermostating must preserve its
297 canonical form. We first describe the rather obvious *uncon-*
298 *strained case*, where we introduce a “primitive thermostating
299 operation” involving a one-dimensional velocity update, and
300 analyze when a sequence of operations requires sequential
301 application and when it can be allowed to be applied in parallel.
302 Then we consider the *constrained case*, first describing the
303 action of constraint routines using a similar matrix notation,
304 followed by a formulation of the canonical equipartition in a
305 constrained system.

306 **4.1. The Unconstrained Case.** Before discussing our
307 solution to the problem of correct thermostating in the

presence of constraints we will introduce a more general
notation for the thermostats introduced in Section 2.

In this paper we are interested in expressing equations using
Cartesian coordinates. There are n particles, $i = 1 \dots n$, and we
will assume three spatial coordinates although this is not
essential. To present the results in their full generality we will
adopt the following matrix notation:

1. \mathbf{x} is a $3n$ dimensional 1-column matrix representing the
3n coordinates of \mathbf{r}_i , $i = 1 \dots n$.
2. \mathbf{v} is a $3n$ dimensional 1-column matrix representing the
3n coordinates of $\dot{\mathbf{r}}_i$, $i = 1 \dots n$.
3. \mathbf{M} is a $3n \times 3n$ square matrix with $m_1, m_1, m_1, m_2, m_2, m_2, \dots, m_n, m_n, m_n$ along its diagonal.

We will consider the following thermostating operation:

$$\mathbf{v}' = (\mathbf{I} - \mathbf{F})\mathbf{v} + \mathbf{G}\xi \quad (18)$$

where ξ is a column vector with normally distributed random
numbers with mean 0 and covariance matrix \mathbf{I} . Here the
matrices \mathbf{F} and \mathbf{G} do not depend on \mathbf{v} .

The equilibrium distribution of velocities is the Maxwell–
Boltzmann distribution. This is a Gaussian distribution with
covariance matrix

$$\langle \mathbf{v}\mathbf{v}^T \rangle = k_B T \mathbf{M}^{-1} \quad (19)$$

Since adding Gaussian variables results in a stochastic variable
that is itself normally distributed, also \mathbf{v}' as computed by eq 18
is a Gaussian variable. This means that it is fully specified by its
covariance matrix (and its mean). The thermostat has the
Maxwell–Boltzmann distribution as invariant distribution if the
covariance matrix of \mathbf{v}' is also given by eq 19. This implies a
relation between \mathbf{F} and \mathbf{G} , namely,

$$k_B T \mathbf{M}^{-1} = (\mathbf{I} - \mathbf{F})k_B T \mathbf{M}^{-1} (\mathbf{I} - \mathbf{F}^T) + \mathbf{G}\mathbf{G}^T$$

$$\mathbf{G}\mathbf{G}^T = k_B T (\mathbf{F}\mathbf{M}^{-1} + \mathbf{M}^{-1}\mathbf{F}^T - \mathbf{F}\mathbf{M}^{-1}\mathbf{F}^T) \quad (20)$$

This relation can be easily solved for \mathbf{G} if, for example, \mathbf{F} and
 \mathbf{M}^{-1} are diagonal matrices. This is the case in simple Langevin
dynamics. But in other case, especially DPD and the Lowe–
Andersen thermostat, where pair-interactions are considered \mathbf{F}
is nondiagonal. In principle, \mathbf{G} can always be found by applying
Cholesky decomposition. This is, however, computationally
very expensive.

The relation can, however, be easily obeyed if \mathbf{G} is a one-
dimensional column vector, such that ξ is in fact a single
random number, and \mathbf{F} is a square matrix of rank one. We will
name this case where only one random number is needed a
primitive thermostating operation. Instead of using a matrix \mathbf{G}
with a rank bigger than 1 we will use a sequence of primitive
thermostating operations where each \mathbf{G} is a $3n \times 1$ matrix, that
is, a column vector. We will denote such a column vector at
step k in the sequence of primitive thermostating operations as
 \mathbf{g}_k , such that

$$\mathbf{v}_{k+1} = (\mathbf{I} - \mathbf{F}_k)\mathbf{v}_k + \mathbf{g}_k \xi_k \quad (21)$$

Let us perform, say m number of these operations, then: $\mathbf{v}_0 \equiv \mathbf{v}$
and $\mathbf{v}' \equiv \mathbf{v}_m$. To make sure that each of these operations leaves
the unconstrained Maxwell–Boltzmann distribution invariant
we require that, according to eq 20,

$$\mathbf{g}_k \mathbf{g}_k^T = k_B T [\mathbf{F}_k \mathbf{M}^{-1} + \mathbf{M}^{-1} \mathbf{F}_k^T - \mathbf{F}_k \mathbf{M}^{-1} \mathbf{F}_k^T] \quad (22)$$

361 which can be used to check or construct specific forms of valid
362 primitive thermostating operations.

363 For example, a simple Langevin damping on one Cartesian
364 degree of freedom (which we can number 1 without loss of
365 generality) yields a matrix \mathbf{F}_k with one value $F_{11} = f_k$ and zero
366 otherwise; application of eq 22 immediately shows that \mathbf{g}_k is a
367 vector with one component g_{11} , with $g_{11}^2 = (k_B T/m_1)(2f - f^2)$. A
368 less trivial example is the *iso*-DPD variant, see eq 5, which—for
369 one Cartesian component numbered 1 for particle i and 2 for
370 particle j —reads

$$\begin{aligned} v_1' &= v_1 + \frac{\mu}{m_1} [(1-f)(v_1 - v_2) + g\xi] \\ v_2' &= v_2 - \frac{\mu}{m_2} [(1-f)(v_1 - v_2) + g\xi] \end{aligned} \quad (23)$$

372 with $g^2 = f(2-f)k_B T/\mu$. In matrix notation this is equivalent to
373 eq 21 with

$$\mathbf{F} = \mu f \mathbf{M}^{-1} \begin{pmatrix} 1 & -1 \\ -1 & 1 \end{pmatrix}; \quad \mathbf{g} = g \mu \mathbf{M}^{-1} \begin{pmatrix} 1 \\ -1 \end{pmatrix} \quad (24)$$

375 which fulfills eq 22.

376 More generally, requirement eq 22 is obeyed for

$$\mathbf{F}_k = f_k \frac{\mathbf{g}_k \mathbf{g}_k^T \mathbf{M}}{\mathbf{g}_k^T \mathbf{M} \mathbf{g}_k}, \quad \text{where } \mathbf{g}_k^T \mathbf{M} \mathbf{g}_k = f_k (2 - f_k) k_B T \quad (25)$$

378 which can be confirmed by back-substitution. It is easily verified
379 that \mathbf{F} and \mathbf{g} of the *iso*-DPD example given above in eq 24,
380 fulfill eq 25.

381 If the primitive thermostating operations are carried out
382 sequentially, the Maxwell–Boltzmann distribution is preserved
383 throughout the sequence. Sequential operation means that each
384 operation is completed (both damping and noise have been
385 applied) before the next operation starts; parallel operation
386 means that the damping is applied to all involved particles, after
387 which the total noise is added. Sequential operation is not
388 needed in all cases; if each particle is touched only once, the
389 primitive operations commute with each other and can be
390 carried out in parallel as well.

391 This special case occurs if all the vectors \mathbf{g}_k obey the
392 orthogonality relation $\mathbf{g}_k^T \mathbf{M} \mathbf{g}_l = 0$ for all $l \neq k$; then also $\mathbf{F}_k \mathbf{F}_l =$
393 $\mathbf{0}$. This orthogonality condition is, for example, obeyed if the
394 entry in \mathbf{g}_k for a specific particle index is nonzero only for one k -
395 value (or never), that is, as each velocity coordinate is touched
396 by the thermostat not more than once. This is commonly the
397 case in Andersen and Langevin types of thermostats where
398 individual particles are thermostated.

399 In the case the orthogonality conditions hold we can define
400 an overall

$$\mathbf{F} = \sum_k \mathbf{F}_k \quad \text{and} \quad \mathbf{G} = [\mathbf{g}_1, \mathbf{g}_2, \dots] \quad (26)$$

402 Now the primitive thermostating operations commute and the
403 thermostating need not be applied sequentially but can be
404 applied in parallel. If the orthogonality condition is not obeyed
405 it is hard to give explicit forms of \mathbf{F} and \mathbf{G} as used in eq 18. In
406 practice no explicit form is created or needed, but the primitive
407 thermostat operations are performed sequentially such as
408 indicated in eq 21.

409 A second special case is when we consider the infinitesimal
410 case $f_k \rightarrow \nu_k dt$. In this case we find (in sloppy notation) that

$$\begin{aligned} \mathbf{F}_k &= (\nu_k dt) \mathbf{M}^{-1} \mathbf{u}_k \mathbf{u}_k^T \quad \text{and} \quad \mathbf{g}_k \\ &= \sqrt{2k_B T \nu_k dt} \mathbf{M}^{-1} \mathbf{u}_k, \quad \text{with } \mathbf{u}_k^T \mathbf{M}^{-1} \mathbf{u}_k \\ &= 1. \end{aligned} \quad (27) \quad 411$$

here the direction vector, \mathbf{u}_k , is normalized by using the inverse
412 mass-matrix as “metric”. In the infinitesimal limit the result will
413 be independent of the sequence of primitive operations, So, in
414 this infinitesimal case eq 26 holds. Clearly, this additivity can
415 break down when going to finite time steps. 416

In a more formal mathematical treatment the combination of
417 time-step and Gaussian, $(dt)^{1/2} \xi_k$, will be denoted as an
418 infinitesimal increment of the Wiener process dW_k . In this case
419 we get 420

$$\mathbf{M} d\mathbf{v}_k = -\nu_k \mathbf{u}_k \mathbf{u}_k^T \mathbf{v}_k dt + \sqrt{2k_B T \nu_k} \mathbf{u}_k dW_k \quad (28) \quad 421$$

The time integration over a finite time-step, Δt , in this case
422 gives explicit expressions for \mathbf{F}_k and \mathbf{g}_k , as 423

$$\begin{aligned} \mathbf{F}_k &= (1 - \exp(-\nu_k \Delta t)) \mathbf{M}^{-1} \mathbf{u}_k \mathbf{u}_k^T \quad \text{and} \quad \mathbf{g}_k \\ &= \sqrt{k_B T (1 - \exp(-2\nu_k \Delta t))} \mathbf{M}^{-1} \mathbf{u}_k \end{aligned} \quad (29) \quad 424$$

which obey relation eq 25, as expected. Note that these
425 individual primitive operations for finite time steps need to be
426 applied sequentially and not in parallel. In parallel applications
427 eq 26 would be used, but in this case eq 25 is not obeyed
428 (unless the orthogonality condition holds for the \mathbf{u}_k values). 429

In the case of DPD or Langevin dynamics the reasoning runs
430 in the opposite direction. There is a stochastic differential
431 equation that needs to be integrated. Now, one can split this
432 equation into primitive parts. Then sequentially a discrete finite
433 time-step approximation for each part is made, and they are
434 applied sequentially. This is usually called an operator-splitting
435 scheme.^{13,18} If each part obeys the correct fluctuation–
436 dissipation relation eq 25, then sequential application as in eq
437 18 yields an invariant Maxwell–Boltzmann distribution. Even
438 though an approximation of the dynamics is used, the
439 equilibrium properties are fully correct. For example, Peters¹⁰
440 proposed two possible forms for \mathbf{F}_k for the DPD case, of which
441 one corresponds to eq 29. 442

For Lowe–Andersen and DPD type thermostats pairs of
443 particles are thermostated and commonly a specific particle
444 participates in multiple pairs. Therefore, in this case, the
445 sequential application is essential. For pairwise interactions one
446 usually requires that the total momentum is conserved. The
447 requirement gives that $\sum_i' [\mathbf{M} \mathbf{g}_k]_i = 0$, where the primed-sum
448 indicates the sum over all indices corresponding to one
449 direction, that is, x , y , or z . A straightforward way to establish
450 this for pairwise interaction is to rewrite $\mathbf{g}_k = \mathbf{M}^{-1} \mathbf{h}_k$, where for
451 the two particle-coordinate indices i and j : $h_{k,i} = -h_{k,j}$, while $h_{k,m}$
452 $= 0$ for $m \neq ij$. The example given in eq 24 is of this form. 453

Note that if one considers the three independent directions
454 x , y , and z sequentially, then the orthogonality condition
455 discussed before is obeyed. Also if we consider orthogonal
456 directions, for example, into the direction $\hat{\mathbf{r}}_j$ and the directions
457 perpendicular to that, this is the case. Therefore, for a pair of
458 particles the three directions can be handled in parallel. The
459 pairwise schemes discussed before have this required form. 460

The pairwise form is a way to introduce conservation of
461 linear momentum, or Galilean invariance, into the thermo-
462 statting. One might wonder how to (locally) conserve angular
463 momentum. Angular momentum is conserved always when 464

465 pairwise forces are applied along the connecting vector. This
466 means it is valid for the original parallel form of DPD, but not
467 when also perpendicular forces are considered, such as in the
468 isotropic or perpendicular DPD implementations.

469 **4.2. Velocity Constraining Expressed as Projection**
470 **Matrix.** We now turn to constrained systems and describe how
471 velocities are constrained by a projection method.

472 Consider a system of n particles with n_c holonomic
473 constraints, given by

$$474 \quad \sigma_s(\mathbf{r}_1, \dots, \mathbf{r}_n) = \sigma_s(\mathbf{x}) = 0 \text{ for } s = 1, \dots, n_c \quad (30)$$

475 These equations define a *constraint manifold*, a $(3N - n_c)$ -
476 dimensional subspace \mathcal{J} , to which the coordinates are
477 restricted at all times. The n_c gradient vectors $\nabla\sigma_s$ are
478 perpendicular to \mathcal{J} at a given reference point; they form a
479 (nonorthogonal) basis spanning the vector space orthogonal to
480 the hyperplane tangential to the constraint manifold. We define
481 the *constraint matrix* \mathbf{C} with components

$$482 \quad C_{si} = \frac{\partial\sigma_s}{\partial x_i} \quad (31)$$

483 Now consider an arbitrary (unconstrained) vector \mathbf{v}^u in $3n$ -
484 dimensional space. We wish to decompose \mathbf{v}^u into a *projection*
485 $\mathbf{v}^c = (\mathbf{I} - \mathbf{P})\mathbf{v}^u$ of \mathbf{v}^u onto the constraint space \mathcal{J} and a
486 remainder $\mathbf{P}\mathbf{v}^u$, which is a vector perpendicular to the constraint
487 hyperspace at the reference point. The vector \mathbf{v}^u could
488 represent the velocities of all particles and construction of the
489 projection $\mathbf{v}^c = (\mathbf{I} - \mathbf{P})\mathbf{v}^u$ would remove components of the
490 velocities that extend beyond \mathcal{J} . This implies that the vector \mathbf{v}^c
491 must be perpendicular to all gradient vectors

$$492 \quad \mathbf{C}\mathbf{v}^c = \mathbf{0} \quad (32)$$

493 These equations are valid for any vector \mathbf{v} , but are in fact the
494 constraint equations for velocities, derived from the fact that
495 the time derivatives of the constraints, eq 30, are zero. Thus,
496 the constrained velocities are subject to

$$497 \quad \forall s: \dot{\sigma}_s(\mathbf{x}) = \sum_i \frac{\partial\sigma_s}{\partial x_i} \dot{x}_i = \sum_i C_{si} v_i^c = 0 \quad (33)$$

498 which is equivalent to eq 32.

499 The projection $(\mathbf{I} - \mathbf{P})$ is realized by a routine `vconstr` with
500 two vectorial arguments

$$501 \quad \mathbf{v}^c = (\mathbf{I} - \mathbf{P})\mathbf{v}^u = \text{vconstr}(\mathbf{v}^u; \mathbf{x}^{\text{ref}}) \quad (34)$$

502 The implementation^{8,14} proceeds as follows, using n_c
503 Lagrange multipliers λ_s . Every velocity is projected onto the
504 hyperplane tangential to the constraint manifold by

$$505 \quad v_i^c = v_i^u - \frac{1}{m_i} \sum_s \lambda_s \frac{\partial\sigma_s}{\partial x_i} \quad (35)$$

506 Each velocity correction has a weight factor equal to the
507 inverse mass of the corresponding particle. This ensures that
508 the total momentum for the particles remains unchanged.
509 Equation 35 reads in matrix notation:

$$510 \quad \mathbf{v}^c = \mathbf{v}^u - \mathbf{M}^{-1}\mathbf{C}^T\lambda \quad (36)$$

511 where λ is determined such that the constraint equations for
512 velocities, eq 32, are satisfied. This implies that

$$513 \quad \mathbf{C}\mathbf{v}^u = \mathbf{C}\mathbf{M}^{-1}\mathbf{C}^T\lambda \quad (37)$$

514 Defining

$$\mathbf{Z} \stackrel{\text{def}}{=} \mathbf{C}\mathbf{M}^{-1}\mathbf{C}^T \quad (38) \quad 515$$

it follows that 516

$$\lambda = \mathbf{Z}^{-1}\mathbf{C}\mathbf{v}^u \quad (39) \quad 517$$

Inserting eq 39 into eq 36, we obtain 518

$$\mathbf{v}^c = \mathbf{v}^u - \mathbf{M}^{-1}\mathbf{C}^T\mathbf{Z}^{-1}\mathbf{C}\mathbf{v}^u = (\mathbf{I} - \mathbf{P})\mathbf{v}^u \quad (40) \quad 519$$

where 520

$$\mathbf{P} \stackrel{\text{def}}{=} \mathbf{M}^{-1}\mathbf{C}^T\mathbf{Z}^{-1}\mathbf{C} \quad (41) \quad 521$$

This establishes that the routine `vconstr` will return the 522
operation $(\mathbf{I} - \mathbf{P})$ applied to its first argument, to within a 523
specified accuracy. The reference vector \mathbf{x}^{ref} is the point on the 524
constraint manifold at which the tangential projection plane is 525
defined. 526

Note that \mathbf{P} , and hence also $\mathbf{I} - \mathbf{P}$, is a *projection matrix*, 527
representing a projection operator. They are equal to their own 528
squares, as is easily verified for \mathbf{P} by using its definition eq 41. 529

While the *linear* projection operator $\mathbf{I} - \mathbf{P}$, as realized, for 530
example, in RATTLE,⁸ is all we need to constrain velocities, the 531
integration of the equations of motion in discrete steps also 532
requires a nonlinear projection of a coordinate displacement 533
from a reference point onto the constraint hypersurface, as 534
realized by SHAKE,¹⁹ SETTLE,²⁰ and LINCS.^{21,22} We shall 535
denote this projection by `xconstr`: 536

$$\mathbf{x}^c = \text{xconstr}(\mathbf{x}^u; \mathbf{x}^{\text{ref}}) \quad (42) \quad 537$$

Figure 3 visualizes the actions of `vconstr` and `xconstr`. 538

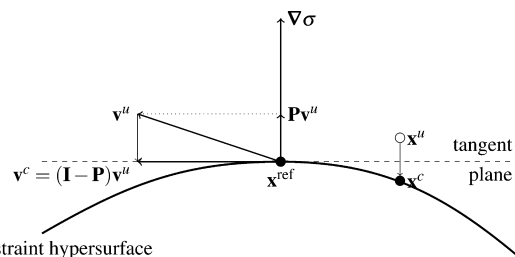


Figure 3. Constraint hypersurface $\mathcal{J}: \sigma = 0$ and the actions of `vconstr` and `xconstr`: projection of a vector \mathbf{v}^u onto the tangent plane to \mathcal{J} at \mathbf{x}^{ref} and projection of a point \mathbf{x}^u onto \mathcal{J} in the direction of the gradient to \mathcal{J} at \mathbf{x}^{ref} .

4.3. The Constrained Canonical Distribution. To 539
correctly resample velocities in the constrained case, we must 540
first ask the question what the canonical distribution is for the 541
constrained velocities. Ryckaert and Ciccotti¹⁴ have shown that 542
a set of unconstrained velocities sampled from a Maxwell– 543
Boltzmann distribution, that is, a set of Gaussian variables with 544
zero mean and correlation matrix given by eq 19, after applying 545
velocity constraints according to eq 34, yields a set of velocities 546
that are samples from the correct canonical probability 547
distribution for constrained systems. This implies that the 548
correlation matrix for constrained velocities is given by 549

$$\langle \mathbf{v}^c \mathbf{v}^{c,T} \rangle = k_B T (\mathbf{I} - \mathbf{P}) \mathbf{M}^{-1} \quad (43) \quad 550$$

This expression follows from working out the correlation 551
matrix for \mathbf{v}^c : 552

$$\langle \mathbf{v}^c \mathbf{v}^{c,T} \rangle = k_B T (\mathbf{I} - \mathbf{P}) \mathbf{M}^{-1} (\mathbf{I} - \mathbf{P}^T) \quad (44) \quad 553$$

and using the relations 554

$$\mathbf{P}\mathbf{M}^{-1} = \mathbf{M}^{-1}\mathbf{P}^T = \mathbf{P}\mathbf{M}^{-1}\mathbf{P}^T \quad (45)$$

556 which follow from the definitions of \mathbf{P} eq 41 and \mathbf{Z} eq 38.
557 Equation 43 is the central theorem on which our paper is based.

558 Equation 43 suggests that the constrained Maxwell–
559 Boltzmann velocity distribution can be generated as follows.
560 First, generate \mathbf{v}^u according to the Gaussian distribution
561 corresponding to the covariance matrix of the unconstrained
562 Maxwell–Boltzmann distribution. This is in practice simple
563 because \mathbf{M} is a diagonal matrix with the particle masses on the
564 diagonal. Next, the unconstrained velocities can be constrained
565 to the correct vector space by performing the projection eq 34:
566 $\mathbf{v}^c = (\mathbf{I} - \mathbf{P})\mathbf{v}^u$.

567 **4.4. The Constrained Case.** The issue of correct
568 thermostating in the presence of constraints is to sample a
569 Gaussian velocity distribution with covariance matrix given by
570 eq 43. From the previous section we arrive at the conclusion
571 that this can be done by first drawing random vectors from the
572 unconstrained Maxwell–Boltzmann distribution and then
573 constraining those vectors.

574 The problem with naive implementations such as discussed in
575 Section 3 is as follows. Suppose that for an initial system the
576 velocities are distributed as they should be, that is, according to
577 eq 43. Next, an unconstrained thermostat is applied. The
578 resulting velocity distribution after that is not equal to the
579 equilibrium unconstrained Maxwell–Boltzmann distribution,
580 because there is still influence of the initial constrained velocity
581 distribution. Neither will the distribution be the constrained
582 one, because the thermostating will not take the constraints
583 into account. If subsequently the constraints are applied using
584 eq 34, the resulting distribution is not equal to the correct
585 constrained Maxwell–Boltzmann distribution.

586 An exception is the case where all particles are fully
587 thermostated, for example, the Andersen thermostat applied
588 to all particles. In that case, after the unconstrained thermo-
589 statting, we obtain the unconstrained Maxwell–Boltzmann
590 distribution. When next applying the constrained we obtain the
591 correct constrained velocity distribution (see Section 4.3)

592 Let us rephrase the main conclusion of the previous section:
593 if we can make sure that we constrain an unconstrained
594 Maxwell–Boltzmann distribution, we obtain the correct
595 constrained one. So, a solution is to first construct an
596 unconstrained Maxwell–Boltzmann distribution out of a
597 constrained one. Next, perform thermostating on the uncon-
598 strained velocities, and last, project these velocities onto the
599 constrained space. We now have a valid thermostat for
600 constrained systems.

601 We will now give our main result, namely, a simple method
602 that does just that. Here it comes:

$$603 \quad \mathbf{v}' = \mathbf{v} + \sqrt{k_B T} \mathbf{P}\mathbf{M}^{-1/2} \boldsymbol{\xi}_1 \quad (46)$$

$$604 \quad \mathbf{v}'' = (\mathbf{I} - \mathbf{F})\mathbf{v}' + \mathbf{G}\boldsymbol{\xi}_2 \quad (47)$$

$$605 \quad \mathbf{v}^{(\text{new})} = (\mathbf{I} - \mathbf{P})\mathbf{v}'' \quad (48)$$

606 where $\boldsymbol{\xi}_1$ and $\boldsymbol{\xi}_2$ are two independent vectors of normally
607 distributed variables with zero mean and unit variance. In this
608 scheme the constrained canonical distribution is the invariant
609 distribution.

610 The important new ingredient, compared to earlier schemes,
611 is the first step. This step adds random components in the
612 constrained directions such that the unconstrained Boltzmann

distribution is recovered, if \mathbf{v} is distributed according to the
constrained canonical distribution eq 43, because 614

$$\begin{aligned} \langle \mathbf{v}'\mathbf{v}'^T \rangle &= \langle \mathbf{v}\mathbf{v}^T \rangle + k_B T \mathbf{P}\mathbf{M}^{-1}\mathbf{P}^T \\ &= k_B T (\mathbf{I} - \mathbf{P})\mathbf{M}^{-1} + k_B T \mathbf{P}\mathbf{M}^{-1}\mathbf{P}^T \\ &= k_B T \mathbf{M}^{-1} \end{aligned} \quad (49) \quad 615$$

In this derivation the properties of \mathbf{P} as stated in eq 45 are used. 616

The second step, eq 47, is the usual thermostating of 617
unconstrained velocities. It usually consists of a sequence of 618
primitive thermostating events, which may be handled in 619
parallel if the events are independent, as discussed in Section 620
4.1. The combined effect of eq 46 and eq 47 is that an 621
unconstrained Maxwell–Boltzmann distribution is sampled 622
(when the initial \mathbf{v} sampled the constrained Maxwell– 623
Boltzmann). So after these two steps we will have a re- 624
equilibrated unconstrained Maxwell–Boltzmann velocity dis- 625
tribution. The last step, eq 48, which is an application of 626
 $\mathbf{v}_{\text{constr}}$, performs the projection of the unconstrained velocities 627
to the correct space. As shown in the previous section, 628
projecting the unconstrained Maxwell–Boltzmann distribution 629
in this way gives the correct constrained distribution. 630

Therefore, the algorithm correctly samples the constrained 631
canonical distribution. If the initial velocity distribution is not 632
the equilibrium one, then the second step, eq 47, causes the 633
final distribution to approach this correct equilibrium 634
distribution. The additional step, compared to previous 635
implementations, is eq 46. This constitutes a generation of 636
Gaussian numbers and a projection step only once per time 637
step (and not once per primitive thermostating event), which 638
involves a very limited computational effort. 639

The new element is the reintroduction of vector components 640
into the constrained directions. By the thermostating these 641
components are mixed in, also in the unconstrained directions. 642
At the end the new velocities pointing into the constrained 643
directions are projected out again. If the f factors are small, say 644
 $O(\Delta t)$, the effect of this mixing in is also small and the major
part of the perpendicular components that were introduced by 645
eq 46 will be removed again by eq 48. In fact, in the 646
infinitesimal limit the equations will reduce to the proper 647
constrained Langevin or DPD equations. 648

In this scheme the thermostating steps occur in the 649
unconstrained velocity space. The reintroduction of the 650
perpendicular components might feel somewhat artificial. 651
One might wonder if it is not possible to fully remain inside 652
the constrained space. In Appendix B we present such a 653
scheme. However, we did not implement this scheme. The 654
reason is that the scheme presented in the appendix needs 655
many projection steps, that is, one or two for every primitive 656
operation. Therefore, in general, it is much more expensive 657
than the method presented in this section. 658

5. INTEGRATION OF THE EQUATIONS OF MOTION

Up to now we focused on the impulsive thermostating. The 659
impulsive thermostating as introduced in this paper only 660
changes velocities and leaves the positions unaltered. In an MD 661
simulation this thermostating needs to be combined with the 662
“conservative part” of the equations of motion. A rigorous 663
integration of the conservative equations of motion conserve 664
energy and obeys, among other things, Liouville’s theorem. 665
This makes the classical Boltzmann distribution invariant under 666
the conservative evolution. 667

668 In practice the equations of motion are discretized. The finite
669 time discretization errors introduce small deviations from the
670 theoretical probability distribution. These deviations are limited
671 by using integrators that leave the underlying “symplectic”
672 structure of classical mechanics equations invariant. In this case
673 the discretized equations actually solve the equations of motion
674 corresponding to a so-called shadow Hamiltonian. A
675 consequence is that also for long times the simulations errors
676 (on average quantities) remain bounded. The most simple type
677 of symplectic integrators are the second-order Verlet schemes.
678 These schemes are highly efficient, and because of the favorable
679 trade-off between accuracy and efficiency, they are commonly
680 used. Also in the presence of constraints generalizations of
681 these integrators have been proved to have the favorable
682 symplectic properties (in the limit of full convergence of the
683 equations that impose the constraints).²³

684 So, the conservative part of the dynamics leaves the
685 Boltzmann equation invariant (to good approximation), while
686 the thermostating leaves the canonical distribution invariant
687 (exactly). During the conservative evolution the system remains
688 on a constant energy hypersurface, while the thermostating
689 causes the energy to change. Therefore, if one is interested in
690 sampling the canonical equilibrium distribution one can
691 alternate purely conservative evolution with impulsive thermo-
692 statting.

693 **5.1. The Conservative Evolution.** For the conservative
694 evolution we propose a velocity-Verlet type of implementation
695 which produces (constrained) equal-time coordinates and
696 velocities, as required for the thermostating step. This implies
697 the use of a RATTLE-type velocity constraining in addition to a
698 SHAKE-type coordinate resetting. Here SHAKE and RATTLE
699 do not refer to the iterative scheme used to impose the
700 constraints—matrix methods may be used—but rather indicate
701 that constraints are applied to positions only or also to
702 velocities. In this case the conservative evolution can be
703 computed as

$$704 \mathbf{v}_{n+1/2}(\lambda_n) \equiv \mathbf{v}_n + \frac{1}{2} \mathbf{M}^{-1} (\mathbf{f}_n + \sum_s \lambda_{ns} \nabla \sigma_s(\mathbf{x}_n)) \Delta t \quad (50)$$

$$705 \mathbf{x}_{n+1}(\lambda_n) \equiv \mathbf{x}_n + \mathbf{v}_{n+1/2}(\lambda_n) \Delta t \quad (51)$$

$$706 \forall s \sigma_s(\mathbf{x}_{n+1}) = 0 \rightarrow \lambda_n \rightarrow \mathbf{x}_{n+1} \rightarrow \mathbf{v}_{n+1/2} \quad (52)$$

$$707 \mathbf{f}_{n+1} = -\nabla U(\mathbf{x}_{n+1}) \quad (53)$$

$$708 \mathbf{v}'_{n+1} = \mathbf{v}_{n+1/2} + \frac{1}{2} \mathbf{M}^{-1} \mathbf{f}_{n+1} \Delta t \quad (54)$$

$$709 \mathbf{v}_{n+1} = (\mathbf{I} - \mathbf{P}) \mathbf{v}'_{n+1} \quad (55)$$

710 In this scheme the first two steps, eq 50 and eq 51, are formal
711 because the Lagrange multipliers indicated by λ_n are still
712 unknown. In the constraining step given by eq 52 these
713 Lagrange multipliers are computed and the conservative
714 constraining forces and new positions are known. These can
715 be used, together, with \mathbf{f}_n to compute the virial contribution to
716 the stress tensor. In the nomenclature of Section 4.2 the first
717 three steps are realized by calling the routine `xconstr` eq 42 and
718 then reconstructing the new midpoint velocities from the
719 constrained positions:

$$720 \mathbf{x}_{n+1} = \text{xconstr} \left(\mathbf{x}_n + \mathbf{v}_n \Delta t + \frac{1}{2} \mathbf{M}^{-1} \mathbf{f}_n (\Delta t)^2; \mathbf{x}_n \right) \quad (56)$$

$$\mathbf{v}_{n+1/2} = (\mathbf{x}_{n+1} - \mathbf{x}_n) / \Delta t \quad (57) \quad 721$$

The last two steps are realized by $\mathbf{v}_{n+1} = \text{vconstr} (\mathbf{v}_{n+1/2} + 1/2 \mathbf{M}^{-1} \mathbf{f}_{n+1} \Delta t; \mathbf{x}_{n+1})$. 722 723

In this scheme the midpoint velocity $\mathbf{v}_{n+1/2}$ is computed. 724 Note that for this velocity $(\mathbf{I} - \mathbf{P}) \mathbf{v}_{n+1/2} = O(\Delta t^2)$ and not 725 exactly equal to zero. We also compute the velocities at integer 726 number of time steps. These velocities are constrained such 727 that $\mathbf{P} \mathbf{v}_{n+1} = 0$ exactly. The determination of fully constrained 728 velocities at integer time steps is what distinguishes velocity- 729 Verlet from Verlet or leapfrog schemes. This property is 730 important for us because our thermostating scheme, that can 731 be applied next, uses the fact that the velocities are constrained. 732 Note that this is different from Goga et al.¹¹ where leapfrog 733 discretizations with a SHAKE-type constraining was used. In 734 that work unconstrained thermostating was applied to $\mathbf{v}_{n+1/2}$ 735 and subsequently the updated positions were constrained. We 736 now know that this procedure can give erroneous results if 737 selected atoms or atom pairs are subjected to impulsive 738 thermostating. 739

For the Andersen and Lowe–Andersen thermostat the 740 impulsive thermostat itself is discrete in nature. Its influence on 741 the dynamics of a system is determined by the frequency the 742 thermostat is applied and the number of particles (or pairs) that 743 are actually thermostated. In other cases, like Langevin 744 dynamics and DPD, the impulsive thermostat provides a 745 discretization of an underlying stochastic differential equation 746 (SDE). For these latter cases one might like to reproduce a 747 dynamics that is as close as possible to the underlying dynamics 748 of the SDE. In this case the time-step size dependence of 749 dynamic quantities such as diffusivity and viscosity should be 750 minimized. 751

5.2. Implementation of the Thermostating. In our 752 method, for the conservative part we need to constrain the 753 position once and the velocity once. Next to that, for the 754 thermostating we need to compute velocity components 755 perpendicular to the constrained space and at the end of the 756 thermostating constrain the velocities again. The basic 757 operation is to project velocities (see Figure 3): either as $\mathbf{v}^\perp = \mathbf{P} \mathbf{v}$ in eq 46, applied to the random vector $\mathbf{v} = \mathbf{M}^{-1/2} \boldsymbol{\xi}$, or 758 as $\mathbf{v}^c = (\mathbf{I} - \mathbf{P}) \mathbf{v}^u$ in eq 48, applied to the modified 759 unconstrained velocities. These are simple operations once 760 the routine `vconstr` eq 34 is available. The projection \mathbf{P} , for 762 example, is computed by $\mathbf{v}^\perp = \mathbf{v} - \text{vconstr}(\mathbf{v}; \mathbf{x}^{\text{ref}})$. 763

5.3. Trotter Expansion. The conservative Verlet or 764 velocity-Verlet scheme discussed above is itself a second- 765 order scheme with respect to the time step. This scheme can be 766 symbolically written as VRV (velocity update, position update, 767 velocity update). 768

If the impulsive thermostat follows from the discretization of 769 a SDE, as for Langevin dynamics or DPD (but not for the 770 Andersen and Lowe–Andersen thermostats), one might worry 771 about the accuracy of the time discretization. For the dissipative 772 and stochastic part of the SDEs the provided thermostating 773 scheme gives a first-order discretization for the dynamics (even 774 though it leaves the equilibrium distribution invariant). This 775 makes the total time evolution only first-order accurate. 776

Let us try to also make the discretization of the stochastic 777 part second order. Note that, in practice, this is often not 778 required. Langevin dynamics and DPD heavily influence the 779 dynamics of a molecular system. This means that, if one is 780 interested in short time transport coefficients, such as diffusion 781 coefficients one will usually not use a thermostat based on this 782

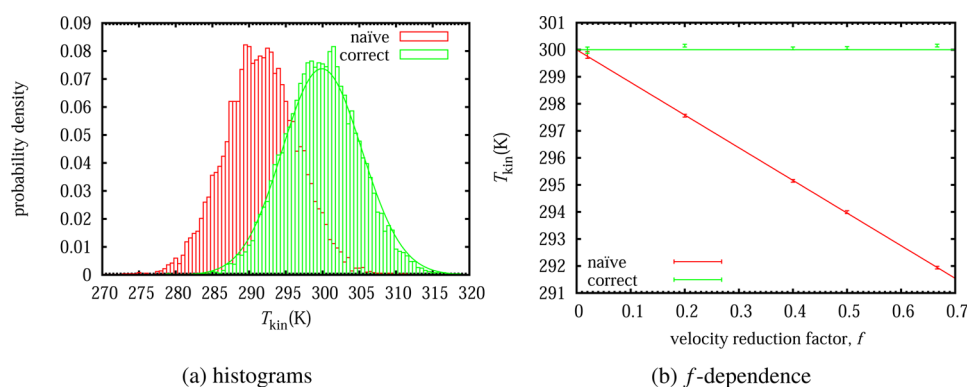


Figure 4. Kinetic temperature is measured for a SPC/E-water simulation with an “iso-DPD” thermostat. The naive thermostating and the correct new thermostating is applied. (a) The histogram for the two methods is compared for $f = 0.67$. The solid green line corresponds to the theoretically expected distribution. (b) The mean temperature is plotted as a function of f . For large values of f the deviation from the thermostat temperature (300 K) is significant.

783 type of dynamics. The impulsive thermostat, however, already
784 makes sure that the equilibrium distribution is invariant.
785 Increasing its time accuracy does not improve this.

786 Having said this, let us assume that we need accurate
787 stochastic dynamics. For an SDE we denote the stochastic
788 dynamics as Ornstein–Uhlenbeck dynamics and denote it as
789 “O”. In Appendix A we discuss this dynamics, its analytical
790 solution, and the construction of a Trotter expansion for the
791 SDE. For unconstrained Langevin dynamics Leimkuhler and
792 Matthews²⁴ have considered several second-order schemes
793 constructed from Trotter expansion. They demonstrated that
794 for Langevin dynamics VRORV performed best. For normal
795 Langevin dynamics the analytical solution can be efficiently
796 evaluated and does not have to be split up (see Appendix A). In
797 other words all primitive thermostating operations can be
798 performed in parallel.

799 This is not the case SDEs that involve pair interaction, such
800 as DPD. As shown in Appendix A in this case numerical
801 evaluation of the Ornstein–Uhlenbeck dynamics is computa-
802 tionally very expensive. For an efficient evaluation of the
803 Ornstein–Uhlenbeck dynamics the dynamics should be split up
804 into individual pair-interactions. A second order Trotter
805 scheme, where an individual primitive thermostat interaction
806 corresponding to pair k is O_k , gives $O \approx O_M \cdots O_2 O_1 O_2 \cdots O_M$.
807 The need for a further Trotter expansion for the Ornstein–
808 Uhlenbeck dynamics is discussed by Serrano et al.¹³ and is also
809 treated in Appendix A.

810 For the case where constraints are present for both Langevin
811 and DPD dynamics the Ornstein–Uhlenbeck dynamics the
812 analytical solution for the O-dynamics can not be efficiently
813 evaluated numerically. A Trotter expansion is possible in this
814 case, see Appendix A.1. However, the price to pay is a large
815 computational overhead because each of the individual
816 primitive thermostating operations involves a projection in
817 this case (see Appendix B). We might follow the method
818 introduced in this paper: of lifting the velocities from the
819 constraint to the unconstrained manifold, next perform primitive
820 thermostating operations, and finally constrain the velocities.
821 In this case the constrained Ornstein–Uhlenbeck dynamics is
822 approximated as $O^c \approx LO_M \cdots O_2 O_1 O_2 \cdots O_M P$ (with L: lifting
823 and P: projection). This is, however, not a true Trotter
824 expansion and second order accuracy is not warranted.

825 Often, when discretization schemes for this type of dynamics
826 are compared one looks at equilibrium quantities like the pair-
827 distribution function (see, for example, ref 13). Note, however,

that no difference will show up whether a Trotter expansion of 828
first or second order is used for the O-dynamics, or whether a 829
proper Trotter expansion for O^c is used or the trick with lifting 830
the velocities to the unconstrained manifold. The reason is that 831
in any of these cases the equilibrium Boltzmann distribution is 832
invariant. The only cause of deviation from equilibrium is the 833
splitting of the conservative dynamics as into R and V. 834
Therefore, one should consider transport properties such as 835
diffusion coefficients to determine the improved time-step 836
dependence of higher order schemes. Because we think the use 837
of improved calculation of transport properties for stochastic 838
dynamics is limited we did not implement the proper 839
constrained second order Trotter expansion with its high 840
computational overhead. 841

6. RESULTS

Two sets of results will be presented. First, we will repeat the 842
simple analysis of a one-dimensional case discussed in Section 843
3. This will illustrate that indeed in this simple case the correct 844
Maxwell–Boltzmann distribution is sampled. Second, we will 845
show water simulations using the similar thermostats as in 846
Goga et al.,¹¹ but with the improved thermostating as 847
discussed in Section 4.4. 848

6.1. One-Dimensional Problem. As a first illustration let 849
us reconsider the first case in Section 3, depicted in Figure 1. 850
With the new scheme the first step is to add thermal noise in 851
the constrained directions. This noise of the relative velocity 852
has variance $(k_B T / \mu)^{1/2}$ with $\mu = (1/2)m$. Next, the 853
unconstrained thermostat is applied. Last, the constraining is 854
applied: 855

$$v'_1 = v_0 - \frac{1}{2} \sqrt{\frac{2k_B T}{m}} \xi_1, v'_2 = v_0 + \frac{1}{2} \sqrt{\frac{2k_B T}{m}} \xi_1 \quad (58) \quad 856$$

$$v''_1 = (1 - f)v'_1 + g\xi_2, v''_2 = v'_2 \quad (59) \quad 857$$

$$v_{\text{cm}} = \frac{1}{2}(v''_1 + v''_2) \quad (60) \quad 858$$

The stationary variance can be computed by equating $\langle v_{\text{cm}}^2 \rangle = 859$
 $\langle v_0^2 \rangle$. To compute the value for $\langle v_{\text{cm}}^2 \rangle$ the properties of the 860
Gaussian variables: $\langle \xi_i^2 \rangle = 1$, $\langle v_0 \xi_i \rangle = 0$ and $\langle \xi_i \xi_j \rangle = 0$, for $i \neq j$ 861
should be used. The value of g is again related to f by means of 862
eq 3. 863

Table 1. Diffusion Coefficients [10^{-9} m²/s] of Water at 298 K for Different Thermostatting Schemes

τ_t [ps]	ISO-1 ^a	ISO-10 ^a	ISO-20 ^a	MD ^b	SD ^c
1	2.622 ± 0.0834	2.417 ± 0.028	2.160 ± 0.007	2.602 ± 0.246	2.352 ± 0.07
0.1	2.250 ± 0.1534	1.181 ± 0.053	0.711 ± 0.002	2.493 ± 0.004	1.269 ± 0.02
0.01	1.092 ± 0.0504	0.212 ± 0.013	0.146 ± 0.007	2.504 ± 0.087	0.202 ± 0.00
0.005	0.690 ± 0.0011	0.147 ± 0.012	0.110 ± 0.000	2.542 ± 0.072	0.103 ± 0.00
0.004	0.560 ± 0.0082	0.112 ± 0.011	0.107 ± 0.001	2.587 ± 0.007	0.079 ± 0.00

^aISO- x is the iso-DPD thermostat with x pair-interactions per particle. ^bMD: global Berendsen thermostat. ^cSD: stochastic Berendsen-van Gunsteren thermostat.

864 From this analysis we find that $\langle v_{\text{cm}}^2 \rangle = k_B T / 2m$, which
865 means that the computed kinetic temperature equals the
866 imposed temperature of the heat bath ($T_{\text{kin}} = T$). We leave it up
867 to the reader to reexamine the second case discussed in Section
868 3. Also in this case, as expected, the correct temperature is
869 recovered.

870 **6.2. Water Simulations.** In this section we reexamine the
871 constrained water simulations reported by Goga et al.¹¹ The
872 temperature is examined for a simulation of 1024 water
873 molecules using the SPC/E model²⁵ where all bond lengths and
874 angles were constrained. A time step of $\Delta t = 2$ fs was used in all
875 computations.

876 The thermostatting was performed with the isotropic DPD-
877 like thermostat¹¹ where one pair per particle per time-step was
878 chosen. The velocity update is as given by eq 23. Note,
879 however, that the velocity reduction factor is position
880 dependent. So in eq 23 substitute $f \rightarrow f \max(1 - r/r_c, 0)$,
881 with a cutoff of $r_c = 1.2$ nm. This thermostat was implemented
882 in both the “naive” way, as outlined in Goga et al., and the
883 “correct” way as outlined in the current paper. In Figure 4
884 results for the kinetic temperatures as a function of the f -factor
885 are presented. When using the correct thermostatting
886 procedure the measured kinetic temperature equals the one
887 of the heat bath, that is, 300 K, whereas for the naive
888 implementation there is an erroneous large f -dependence.

889 In Table 1 a comparison of diffusion coefficients computed
890 by different thermostats is presented. The parameter τ_t gives
891 the relaxation time scale set in Gromacs.²⁶ For the iso-DPD
892 thermostat the relation with the velocity reduction factor is $\tau_t =$
893 $\Delta t / f$. For a global thermostat like the Berendsen thermostat the
894 influence on the computed diffusion coefficient is little. The
895 strength of the iso-DPD thermostat can be reduced by
896 choosing as small f (large τ_t) and a small number of pair-
897 interactions per particle. If the strength is small the diffusion
898 coefficient is nearly unchanged. If the number of interactions is
899 increased and/or τ_t is decreased the influence on the dynamics
900 increases and the diffusion coefficient diminishes.

7. CONCLUSIONS AND DISCUSSION

901 In this paper we discussed the use of so-called impulsive
902 thermostats in the presence of constraints. The most widely
903 used impulsive thermostat is that of Andersen.⁸ It is not widely
904 acknowledged that, in the presence of constraints, this
905 thermostat breaks down if only a limited number of atoms
906 (instead of all) are re-equilibrated. This also occurs for other
907 thermostats, such as Lowe–Andersen,⁹ and impulsive imple-
908 mentations of DPD-type thermostats.^{10,11}

909 We showed using a simple one-dimensional analysis that the
910 problem is real and sometimes severe and we proposed a
911 simple solution for it. This solution is to add velocity
912 components in the constrained directions, next apply the
913 impulsive thermostats to these unconstrained velocities and

914 finally project the velocities back onto the constrained velocity
915 space. This solution was demonstrated to resolve the issue for
916 the simple one-dimensional cases as well as for water
917 simulations previously presented.¹¹

918 An implementation of a full DPD thermostat involving all
919 pairs within a given range, will give rise to a substantial
920 additional computational cost due to the large number of pairs
921 that are subjected to friction and noise. If one is interested in
922 applying accurate local thermostatting in a Galilean-invariant
923 manner, but is not as much interested in full DPD dynamics,
924 one might opt for the approach of Goga et al.,¹¹ who apply
925 thermostatting to only one or a limited number of pairs per
926 particle. In this way the extra overhead is minimized, while
927 high-quality thermostatting is realized.

928 Using the impulsive schemes presented here, temperature
929 deviations can only be caused by the conservative part of the
930 equations of motion. We have advocated the use of the
931 velocity-Verlet scheme, which uses a Trotter-splitting of the
932 VRV type (where V is a conservative velocity update over $1/2\Delta t$
933 and R a coordinate update over Δt) and which is second-
934 order accurate in Δt , combined with a single application of a
935 sequence of primitive thermostatting operations to the
936 velocities between two conservative steps. This amounts to
937 an asymmetric VRVO scheme, where O is the impulsive
938 velocity update over Δt . While the thermostatting is accurate
939 and the overall scheme remains symplectic, the thermostatting
940 will partly destroy the second-order precision in the dynamical
941 evolution. It might be expected that symmetric impulsive
942 schemes, such as RVOVR or OVRVO, have a higher dynamical
943 accuracy, but this remains to be investigated. The addition of
944 thermal noise deteriorates dynamical precision in any case.
945 Properties that need to be addressed are the time-step
946 dependence of quantities that depend on time correlations,
947 like transport properties such as diffusivity and viscosity.

948 An issue, in this respect, is that the currently implemented
949 impulsive thermostat with constraints can not be (fully) splitted
950 as is needed for the Trotter expansion. In Appendix A.1 we
951 present an implementation that can be splitted and is suited for
952 Trotter expansion. However, this implementation will be
953 computationally more expensive because many more projection
954 steps need to be performed (see Appendix B). It remains to be
955 investigated if in certain cases there is a benefit of using the
956 more complicated version of rigorous impulsive constrained
957 thermostatting.

APPENDIX A. ORNSTEIN–UHLENBECK DYNAMICS

958 The full dynamics of a system evolving according to Langevin
959 dynamics can be symbolically written as

$$\dot{\mathbf{z}} = \mathcal{L}\mathbf{z} = (\mathcal{L}_V + \mathcal{L}_R + \mathcal{L}_O)\mathbf{z} \quad (61)$$

960 where the state \mathbf{z} denotes all particle positions and velocities.
961 The formal solution is $\mathbf{z}(t) = \exp[\mathcal{L}t]\mathbf{z}(0)$. In a Trotter
962

964 expansion the Liouvillian is split up into parts, and the solutions
 965 $\exp[\mathcal{L}_{\text{sub}}t]$ are used as building blocks of a numerical
 966 approximation. To be able to do this, clearly, the solution of
 967 the subdynamics corresponding to \mathcal{L}_{sub} should be analytically
 968 solvable. This type of splitting for unconstrained ordinary
 969 Langevin equations has been considered, for example, by Bussi
 970 and Parrinello²⁷ and by Leimkuhler and Matthews.²⁴
 971 In eq 61 the Liouville operator corresponding to conservative
 972 velocity updates and position updates are

$$973 \quad \mathcal{L}_{\mathbf{v}} = \mathbf{M}^{-1}\mathbf{f}\frac{\partial}{\partial\mathbf{v}}, \text{ and } \mathcal{L}_{\mathbf{r}} = \mathbf{v}\frac{\partial}{\partial\mathbf{r}} \quad (62)$$

974 If the mass matrix, \mathbf{M} , and the forces, \mathbf{f} , only depend on
 975 positions (and not on velocities) the time evolution
 976 corresponding to these sub-Liouvillians can be solved analyti-
 977 cally to give

$$978 \quad \dot{\mathbf{z}} = \mathcal{L}_{\mathbf{v}}\mathbf{z} \rightarrow \mathbf{v}(t) = \mathbf{v}(0) + \mathbf{M}^{-1}\mathbf{f}t, \mathbf{r}(t) = \mathbf{r}(0) \quad (63)$$

$$979 \quad \dot{\mathbf{z}} = \mathcal{L}_{\mathbf{r}}\mathbf{z} \rightarrow \mathbf{v}(t) = \mathbf{v}(0), \mathbf{r}(t) = \mathbf{r}(0) + \mathbf{v}t \quad (64)$$

980 For example, the Trotter-expansion $\exp[(1/2)\mathcal{L}_{\mathbf{v}}\Delta t]\exp[\mathcal{L}_{\mathbf{r}}\Delta t]$
 981 $\exp[(1/2)\mathcal{L}_{\mathbf{v}}\Delta t]$ corresponds to the velocity-Verlet
 982 algorithm. In the main text we indicate this scheme as VRV.
 983 The dynamics of the Ornstein–Uhlenbeck part of the
 984 Langevin dynamics, \mathcal{L}_o , corresponds to the stochastic differ-
 985 ential equation

$$986 \quad \mathbf{M}d\mathbf{v} = -\boldsymbol{\gamma}\mathbf{v}dt + \sqrt{2k_{\text{B}}T\boldsymbol{\gamma}}d\mathbf{W}_i, d\mathbf{x} = \mathbf{0} \quad (65)$$

987 where each component of the vector \mathbf{W}_i is a Wiener process. If
 988 the mass matrix, \mathbf{M} , and the friction matrix, $\boldsymbol{\gamma}$, only have a
 989 positional dependence the analytical solution is

$$990 \quad \mathbf{v}(t) = \exp[-\mathbf{M}^{-1}\boldsymbol{\gamma}t]\mathbf{v}(0) \\ + \sqrt{k_{\text{B}}T(\mathbf{I} - \exp[-2\mathbf{M}^{-1}\boldsymbol{\gamma}t])\mathbf{M}^{-1}}\boldsymbol{\xi}, \mathbf{x}(t) \\ = \mathbf{x}(0) \quad (66)$$

991 Here $\boldsymbol{\xi}$ is a vector of independent Gaussian variables each with
 992 mean 0 and variance 1. In terms of the update scheme given by
 993 eq 18 we find that

$$994 \quad \mathbf{F} = \mathbf{I} - \exp[-\mathbf{M}^{-1}\boldsymbol{\gamma}t] \text{ and } \mathbf{G} \\ = \sqrt{k_{\text{B}}T(\mathbf{I} - \exp[-2\mathbf{M}^{-1}\boldsymbol{\gamma}t])\mathbf{M}^{-1}} \quad (67)$$

995 Because these matrices obey eq 20 the update leaves the
 996 Maxwell–Boltzmann distribution invariant (as it should).

997 For ordinary Langevin dynamics the mass matrix \mathbf{M} and the
 998 friction matrix $\boldsymbol{\gamma}$ are diagonal (and possible position depend-
 999 ent). In this case the rigorous solution can be easily computed.
 1000 This is different in the case where these matrices are
 1001 nondiagonal, but remain sparse. Still, in this case the solution
 1002 can be computed numerically, but computing the exponents
 1003 (and square-root) of the matrices is computationally demand-
 1004 ing. This can be probably achieved by applying Krylov subspace
 1005 methods such as implemented in Expokit.²⁸

1006 To avoid this expensive computation, but still retain valuable
 1007 properties one can try to decompose \mathcal{L}_o further in sub-
 1008 Liouvillians that can be solved analytically. To obtain a second-
 1009 order Trotter expansion we can split-off one sub-Liouvillian at a
 1010 time. If we define $\mathcal{L}_{r-o}^{(k)}$ as the remaining Ornstein–Uhlenbeck
 1011 operator with k sub-Liouvillians split of we find, recursively, for
 1012 a second order expansion,

$$\exp[\mathcal{L}_{r-o}^{(k)}t] \approx \exp\left[\frac{1}{2}\mathcal{L}_o^{(k)}t\right] \exp[\mathcal{L}_{r-o}^{(k+1)}t] \exp\left[\frac{1}{2}\mathcal{L}_o^{(k)}t\right] \quad (68) \quad 1013$$

where $\mathcal{L}_{r-o}^{(0)} = \mathcal{L}_o$ and $\mathcal{L}_{r-o}^{(3M)} = 0$. 1014

If we continue up to the point that all Ornstein–Uhlenbeck
 sub-Liouvillians are split we find sequence of changes of
 velocities of each pair according to eq 66. So, in symbolic
 notation we have $O \approx O_{3M} \dots O_2 O_1 O_1 O_2 \dots O_{3M}$. Note that we find
 that the final result will be different depending on the
 numbering of the pairs. However, any of these alternatives is
 a valid second-order expansion. 1021

A way to split up the Ornstein–Uhlenbeck Liouville operator
 is to decompose the friction matrix as 1023

$$\boldsymbol{\gamma} = \sum_k \boldsymbol{\gamma}_k \text{ with } \boldsymbol{\gamma}_k = \nu_k \mathbf{u}_k \mathbf{u}_k^T \text{ and } \mathbf{u}_k^T \mathbf{M}^{-1} \mathbf{u}_k = 1. \quad (69) \quad 1024$$

In this case each subfriction matrix has rank 1. The
 normalization of \mathbf{u} is such that the matrix exponential in eq
 67 (with $\boldsymbol{\gamma} \rightarrow \boldsymbol{\gamma}_k$ can be easily evaluated. For $\boldsymbol{\gamma}_k$ eq 67 reduces eq
 29, which is an expression that can be easily evaluated
 numerically. 1029

This situation of a nondiagonal friction matrix typically arises
 in the case of DPD dynamics. In this case the Ornstein–
 Uhlenbeck dynamics is 1032

$$m_i d\mathbf{v}_i = - \sum_j \boldsymbol{\gamma} \mathbf{f}(r_{ij})(\mathbf{v}_i - \mathbf{v}_j) + \sum_{j \neq i} \sqrt{2k_{\text{B}}T\boldsymbol{\gamma} \mathbf{f}(r_{ij})} d\mathbf{W}_{ij} \quad (70) \quad 1033$$

In this equation the boldface indicates the three spatial
 directions and the subscripts correspond to particle indices.
 So, we can imagine the big matrix $\boldsymbol{\gamma}$ as in eq 65 to consist of $3 \times$
 3 blocks with values of $-\boldsymbol{\gamma} \mathbf{f}(r_{ij})$ on the ij off-diagonal block and
 of $\boldsymbol{\gamma} \sum_{j \neq i} \mathbf{f}(r_{ij})$ on the diagonal ii -block. The mass matrix is
 diagonal. In this formula there is one independent Wiener
 process for each pair (in each spatial direction), and $\mathbf{W}_{ij} = -\mathbf{W}_{ji}$
 (such that momentum is conserved). 1041

Instead of computing complicated matrix functions we
 further subdivide \mathcal{L}_o by considering each pair interaction
 separately. If we denote $\mathcal{L}_o^{(k)}$ as the Liouvillian corresponding to
 pair the pair indicated by the label k (say k corresponds to the
 pair ij). Then $\mathcal{L}_o = \sum_k \mathcal{L}_o^{(k)}$, that is, the sum over all pairs. In
 that case an $\mathcal{L}_o^{(k)}$ would correspond to the dynamics 1047

$$m_i d\mathbf{v}_i = -\boldsymbol{\gamma} \mathbf{f}(r_{ij})(\mathbf{v}_i - \mathbf{v}_j) + \sqrt{2k_{\text{B}}T\boldsymbol{\gamma} \mathbf{f}(r_{ij})} d\mathbf{W}_k \quad (71) \quad 1048$$

$$m_j d\mathbf{v}_j = -\boldsymbol{\gamma} \mathbf{f}(r_{ij})(\mathbf{v}_j - \mathbf{v}_i) - \sqrt{2k_{\text{B}}T\boldsymbol{\gamma} \mathbf{f}(r_{ij})} d\mathbf{W}_k \quad (72) \quad 1049$$

This system has the same shape as eq 65 only in this case the
 matrix $\boldsymbol{\gamma}$ only has nonzero entries for the 3×3 blocks
 corresponding particles i and j . 1052

The only potential issue is that the 3×3 matrix $\mathbf{f}(r_{ij})$ might
 need to be decomposed. Usually, however, its shape is either
 isotropic $\mathbf{f}(r_{ij}) = f_{\text{iso}}(r_{ij})\mathbf{I}$ or anisotropic of the form $\mathbf{f}(r_{ij}) = f_{\parallel}(r_{ij})$
 $\hat{\mathbf{r}}_{ij} \hat{\mathbf{r}}_{ij}^T + f_{\perp}(r_{ij})(\mathbf{I} - \hat{\mathbf{r}}_{ij} \hat{\mathbf{r}}_{ij}^T)$. In both cases the matrix is already
 effectively diagonal and the computation of matrix functions is
 trivial. To cleanly connect to the primitive thermostating
 operations we can consider the three spatial directions
 separately. If we do this then every index k indicates a pair
 and direction combination. This is there are M pairs the index k
 runs from 1 to $3M$. Note that in the usual case of DPD, the
 primitive operations in the three directions can be applied in
 parallel without causing issues. 1064

1065 As a concrete example let us consider the primitive
1066 thermostatting operation between particles 1 and 2 in the
1067 parallel direction for anisotropic DPD. In that case

$$\mathbf{u} = \sqrt{\mu} \begin{pmatrix} \hat{\mathbf{r}}_{12} \\ -\hat{\mathbf{r}}_{12} \end{pmatrix}, \text{ and } \nu = (\gamma/\mu)f_{\parallel}(r_{12}) \quad (73)$$

1069 Here the reduced mass, μ , occurs to ensure that $\mathbf{u}^T \mathbf{M}^{-1} \mathbf{u} = 1$.
1070 According to the analytical solution, eq 29, the analytical
1071 primitive thermostat operation is thus characterized by

$$\mathbf{F} = (1 - \exp(-\nu \Delta t)) \begin{pmatrix} (\mu/m_1)\hat{\mathbf{r}}_{12}\hat{\mathbf{r}}_{12}^T & -(\mu/m_1)\hat{\mathbf{r}}_{12}\hat{\mathbf{r}}_{12}^T \\ -(\mu/m_2)\hat{\mathbf{r}}_{12}\hat{\mathbf{r}}_{12}^T & (\mu/m_1)\hat{\mathbf{r}}_{12}\hat{\mathbf{r}}_{12}^T \end{pmatrix} \quad (74)$$

$$\mathbf{g} = \sqrt{\mu k_B T (1 - \exp(-2\nu \Delta t))} \begin{pmatrix} \hat{\mathbf{r}}_{12}/m_1 \\ -\hat{\mathbf{r}}_{12}/m_2 \end{pmatrix} \quad (75)$$

1074 **A.1. Constrained Ornstein–Uhlenbeck Dynamics.** If
1075 we apply constraints the Ornstein–Uhlenbeck dynamics
1076 changes to

$$\mathbf{M} d\mathbf{v} = -\gamma \mathbf{v} dt + \sqrt{k_B T \gamma} d\mathbf{W}_t - \mathbf{C}^T d\lambda, \quad d\mathbf{x} = \mathbf{0} \quad (76)$$

1078 where $d\lambda$ is such that $\mathbf{C}\mathbf{v} = \mathbf{0}$. This gives

$$\begin{aligned} \mathbf{M} d\mathbf{v} &= -\gamma^c \mathbf{v} dt + \sqrt{k_B T \gamma^c} d\mathbf{W}_t^c \text{ with } \gamma^c \\ &= (\mathbf{I} - \mathbf{P})^T \gamma (\mathbf{I} - \mathbf{P}) \end{aligned} \quad (77)$$

1080 If we derive the decomposition for the constrained case from
1081 the unconstrained one, that is, take $\gamma_k^c = (\mathbf{I} - \mathbf{P})^T \gamma_k (\mathbf{I} - \mathbf{P})$, we
1082 find with $\gamma_k^c = \nu_k^c \mathbf{u}_k^c \mathbf{u}_k^{cT}$

$$\nu_k^c = (\mathbf{u}_k^T (\mathbf{I} - \mathbf{P}) \mathbf{M}^{-1} \mathbf{u}_k) \nu_k \text{ and } \mathbf{u}_k^c = \frac{(\mathbf{I} - \mathbf{P}^T) \mathbf{u}_k}{\sqrt{\mathbf{u}_k^T (\mathbf{I} - \mathbf{P}) \mathbf{M}^{-1} \mathbf{u}_k}} \quad (78)$$

1084 With these definitions the analytical solution again follows from
1085 eq 29. Note that, when constructing \mathbf{u}_k^c from \mathbf{u}_k , a factor is
1086 introduced that ensures $\mathbf{u}_k^{cT} \mathbf{M}^{-1} \mathbf{u}_k^c = 1$. While in the solution of,
1087 for example, the DPD equations \mathbf{u}_k has two nonzero entries,
1088 namely, for the two particles in pair k , the projection makes that
1089 \mathbf{u}_k^c all particles connected by constrains to either of these
1090 particles are involved. This issue will be discussed in a more
1091 general setting below.

1092 ■ APPENDIX B. PRIMITIVE ONE-STEP OPERATIONS 1093 FOR CONSTRAINED IMPULSIVE 1094 THERMOSTATting

1095 Suppose we would like to produce correct impulsive thermo-
1096 statting in the presence of constraints without the need of
1097 (temporary) introducing velocity components in unconstrained
1098 directions. Let us write such a scheme for a primitive (one-
1099 dimensional) thermostatting operation again (cf. eq 21) as

$$\mathbf{v}' = (\mathbf{I} - \mathbf{F}^c) \mathbf{v} + \mathbf{g}^c \xi \quad (79)$$

1101 but now keeping both $\mathbf{F}^c \mathbf{v}$ and \mathbf{g}^c within the constraint
1102 hyperspace. This implies that $\mathbf{P} \mathbf{F}^c \mathbf{v} = \mathbf{P}^c \mathbf{g}^c = \mathbf{0}$. In this case the
1103 covariance matrix should correspond to the constrained
1104 canonical distribution eq 43, such that

$$\begin{aligned} k_B T (\mathbf{I} - \mathbf{P}) \mathbf{M}^{-1} &= k_B T (\mathbf{I} - \mathbf{F}^c) (\mathbf{I} - \mathbf{P}) \mathbf{M}^{-1} (\mathbf{I} - \mathbf{F}^{cT}) \\ &+ \mathbf{g}^c \mathbf{g}^{cT} \end{aligned} \quad (80) \quad 1105$$

which can be rewritten as (cf. eq 22) 1106

$$\begin{aligned} \mathbf{g}^c \mathbf{g}^{cT} &= k_B T [\mathbf{F}^c (\mathbf{I} - \mathbf{P}) \mathbf{M}^{-1} + (\mathbf{I} - \mathbf{P}) \mathbf{M}^{-1} \mathbf{F}^{cT} \\ &- \mathbf{F}^c (\mathbf{I} - \mathbf{P}) \mathbf{M}^{-1} \mathbf{F}^{cT}] \end{aligned} \quad (81) \quad 1107$$

A primitive operation that obeys this relation is, similar to eq 1108
22, 1109

$$\mathbf{F}^c = f \frac{\mathbf{g}^c \mathbf{g}^{cT} \mathbf{M}}{\mathbf{g}^{cT} \mathbf{M} \mathbf{g}^c}, \text{ with } f(2-f) = \frac{\mathbf{g}^{cT} \mathbf{M} \mathbf{g}^c}{k_B T} \quad (82) \quad 1110$$

but under the extra condition that $\mathbf{P} \mathbf{g}^c = \mathbf{0}$. This condition 1111
implies that $\mathbf{P} \mathbf{F}^c = \mathbf{0}$. It is satisfied if \mathbf{g}^c is constructed from an 1112
unconstrained vector \mathbf{g} as 1113

$$\mathbf{g}^c = (\mathbf{I} - \mathbf{P}) \mathbf{g} \quad (83) \quad 1114$$

Equation 82 is very analogous to the one given in eq 25. Its 1115
validity can be checked by back-substitution in eq 81 and using 1116
the identities given in eq 45. 1117

In practice one may proceed as follows: First construct a 1118
vector \mathbf{g} as in an unconstrained case, for example, as given in eq 1119
24 for the one-dimensional *iso*-DPD example. Next, apply the 1120
`vconstr(g)` routine to construct \mathbf{g}^c , followed by a construction 1121
of \mathbf{F}^c according to eq 82. Note that, although projection of the 1122
unconstrained \mathbf{g} gives a result that leaves the constrained 1123
Maxwell–Boltzmann invariant, if one wants to construct a 1124
analytical solution of constrained Ornstein–Uhlenbeck dynam- 1125
ics then substituting eq 78 into eq 29 gives that there is an extra 1126
time-step dependent factor involved. Also note that this 1127
projection step mixes all components that are related to the 1128
thermostated pair through (a sequence of) constraints, thus 1129
loosing the simplicity of the unconstrained thermostatting 1130
event. 1131

Sequential application of these primitive operations gives rise 1132
to the constrained canonical distribution. This is achieved 1133
without leaving the constraint hypersurface. Each individual 1134
primitive operation leaves the constrained canonical distribu- 1135
tion invariant. Therefore, these operations, actually the one that 1136
follows from eq 78, can be used in a splitting scheme such as a 1137
higher order Trotter expansion. 1138

The main drawback of this method is that for the 1139
computation of each \mathbf{g}_k^c in a sequence of primitive thermo- 1140
statting operations a projection is needed. It depends on the 1141
molecular system that is being simulated if this is in fact 1142
expensive or not. In general, only one or two particle velocities 1143
would be influenced by the unprojected primitive vector \mathbf{g} . The 1144
constraints, however, create a connected path. If the particles 1145
are “connected” by means of constraints to many other particles 1146
then many velocities need to be updated during the application 1147
of friction and noise. 1148

So in general, if the connectedness is relatively small as in a 1149
water simulation, the extra overhead will be limited. If, however, 1150
the connectedness is large, such as in macromolecule 1151
simulations where all bond lengths and angles are constrained, 1152
the overhead of this scheme compared to the one discussed in 1153
the main body will be huge. 1154

1155 ■ AUTHOR INFORMATION

1156 Corresponding Author

1157 *E-mail: e.a.j.f.peters@tue.nl.

1158 **Notes**

1159 The authors declare no competing financial interest.

1160 ■ **REFERENCES**

- 1161 (1) Ermak, D. L.; Buckholz, H. J. *Comput. Phys.* **1980**, *35*, 169–182.
1162 (2) Allen, M. P.; Tildesley, D. J. *Computer Simulation of Liquids*;
1163 Oxford University Press: New York, 1989.
1164 (3) Frenkel, D.; Smit, B. *Understanding Molecular Simulation*, 2nd ed.;
1165 Prentice Hall: New Jersey, 2001.
1166 (4) Berendsen, H. J. C. *Simulating the Physical World, A Hierarchy of*
1167 *Models for Simulation*; Cambridge University Press: Cambridge, U.K.,
1168 2007.
1169 (5) Van Gunsteren, W. F.; Berendsen, H. J. C.; Rullmann, J. A. C.
1170 *Mol. Phys.* **1981**, *44*, 69–95.
1171 (6) Van Gunsteren, W. F.; Berendsen, H. J. C. *Mol. Phys.* **1982**, *45*,
1172 637–647.
1173 (7) Van Gunsteren, W. F.; Berendsen, H. J. C. *Mol. Simul.* **1988**, *1*,
1174 173–185.
1175 (8) Andersen, H. C. *J. Chem. Phys.* **1980**, *72*, 2384–2393.
1176 (9) Lowe, C. P. *Europhys. Lett.* **1999**, *47*, 145–151.
1177 (10) Peters, E. A. F. *J. Europhys. Lett.* **2004**, *66*, 311–317.
1178 (11) Goga, N.; Rzepiela, A. J.; de Vries, A. H.; Marrink, S. J.;
1179 Berendsen, H. J. C. *J. Chem. Theory Comput.* **2012**, *8*, 3637–3649.
1180 (12) Sivak, D. A.; Chodera, J. D.; Crooks, G. E. *arXiv:1301.3800v2*
1181 *[physics.comp-ph]* **2013**, 1–15.
1182 (13) Serrano, M.; De Fabritiis, G.; Español, P.; Coveney, P. V. *Math.*
1183 *Comput. Simul.* **2006**, *72*, 190–194.
1184 (14) Ryckaert, J.-P.; Ciccotti, G. *Mol. Phys.* **1986**, *58*, 1125–1136.
1185 (15) Vanden Eijnden, E.; Ciccotti, G. *Chem. Phys. Lett.* **2006**, *429*,
1186 310–316.
1187 (16) Kallemov, B.; Miller, G. H. *SIAM J. Sci. Comput.* **2011**, *33*, 653–
1188 676.
1189 (17) Koelman, J. M. V. A.; Hoogerbrugge, P. J. *Europhys. Lett.* **1993**,
1190 *21*, 363–368.
1191 (18) Shardlow, T. *SIAM J. Sci. Comput.* **2003**, *24*, 1267–1282.
1192 (19) Ryckaert, J. P.; Ciccotti, G.; Berendsen, H. J. C. *J. Comput. Phys.*
1193 **1977**, *23*, 327–341.
1194 (20) Miyamoto, S.; Kollman, P. A. *J. Comput. Chem.* **1992**, *13*, 952–
1195 962.
1196 (21) Hess, B.; Bekker, H.; Berendsen, H. J. C.; Fraaije, J. G. E. M. *J.*
1197 *Comput. Chem.* **1997**, *18*, 1463–1472.
1198 (22) Hess, B. *J. Chem. Theory Comput.* **2008**, *4*, 116–122.
1199 (23) Leimkuhler, B. J.; Skeel, R. D. *J. Comput. Phys.* **1994**, *112*, 117–
1200 125.
1201 (24) Leimkuhler, B.; Matthews, C. *Appl. Math. Res. Express* **2013**, *1*,
1202 34–56.
1203 (25) Berendsen, H. J. C.; Grigera, J. R.; Straatsma, T. P. *J. Phys. Chem.*
1204 **1987**, *91*, 6269–6271.
1205 (26) van der Spoel, D.; Lindahl, E.; Hess, B.; van Buuren, A. R.; Apol,
1206 E.; Meulenhoff, P. J.; Tieleman, D. P.; Sijbers, A. L. T. M.; Feenstra, K.
1207 A.; van Drunen R.; Berendsen, H. J. C. *Gromacs User Manual, Version*
1208 *4.5.6*; 2010. <http://www.gromacs.org>.
1209 (27) Bussi, G.; Parrinello, M. *Phys. Rev. E* **2007**, *75*, 056707.
1210 (28) Sidje, R. B. *ACM Trans. Math. Software* **1998**, *24*, 130–156.